

# A NEW METHOD FOR TREE SPECIES ARRANGEMENT IN FARMLAND SHELTERBELTS AND SAND PREVENTION ANALYSIS

## 农田防护林配置及防治风沙效应的新型方法分析

Ph.D. Stud. Deng Jifeng<sup>1,2)</sup>, Prof. Ph.D. Ding Guodong<sup>\*1,2)</sup>, Ph.D. Gao Guanglei<sup>1,2)</sup>, Ph.D. Stud. Gao Lin<sup>3)</sup>

<sup>1)</sup> Yanchi Research Station, School of Soil & Water Conservation, Beijing Forestry University, Beijing / P.R. China;

<sup>2)</sup> Key Laboratory of Soil and Water Conservation and Desertification Combating, Ministry of Education, Beijing Forestry University, Beijing / P.R. China

<sup>3)</sup> Faculty of Forestry and Environmental Management, University of New Brunswick, Fredericton / Canada  
Tel: +8618504508251; E-mail: [dengjifeng1984@gmail.com](mailto:dengjifeng1984@gmail.com)

**Abstract:** Farmland shelterbelts can yield maximum ecological benefits with the smallest occupied area of forests and result in sustainable use of farmland resources. Rapid and efficient planning of farmland shelterbelts at various scales is becoming an urgent task in ecological landscape design. Until now, the problems in studies on farmland shelterbelts combined with wind erosion models are associated with conflicts between scientific and practical requirements. Based on previous research results, a case study was conducted in Yanchi County in north-western China. The primary objectives of this study were to use a new method for the arrangement of tree species and to investigate the effects of sand prevention. In addition, changes in the trends of the input parameters under multiple wind erosion events were analyzed and tested. The results indicated that under a single arrangement of tree species, better shelter protection was provided within the shrub shelterbelt or outside the arbor shelterbelt forest. Under a different arrangement of tree species, shrubs arranged with arbor belts gave little protection on the leeward side. Arbor trees arranged with shrub belts could effectively prevent sand from the windward side, while low trees in the upwind direction provided limited protection. Cumulative percentiles of sand displacement showed that under different arrangements of tree species, the sand prevention benefit was better than that of a single tree species. In addition, the experimental error was less than 3.00% and there was close correlation between percentiles of sand displacement under multiple wind erosion events, indicating a preferable simulation effect.

**Keywords:** farmland shelterbelt, exponential model, summation curve method, wind erosion

### INTRODUCTION

Shelterbelts are artificial barriers used to reduce wind velocity. In history they have been used to protect homes and enhance the agricultural landscape [1]. As an important type of shelterbelts, farmland shelterbelts can increase animal and plant species and enhance the ecological function of agricultural systems. Furthermore, it can protect soils from erosion forms, and boost crop yields [5, 15]. Therefore, the construction of farmland shelterbelts plays a significant role in achieving sustainable development. So far, researches related to the farmland shelterbelt have paid more attention to the structure and protective effects of shelterbelts combined with the existing wind erosion models at a small scale.

Studies on the structure of farmland shelterbelt systems focused mainly on forest structural characteristics and their relationship with meteorological

**摘要:** 农田防护林占森林面积最小却能发挥最大的生态效益, 体现在对农田资源的可持续利用方面。如何在不同尺度上快速而又有效地规划农田防护林是生态景观设计急需解决的命题。目前为止, 对于农田防护林结合现有风蚀模型的研究存在科学性与实用性需求之间的矛盾。本文在前人研究的基础上, 以中国西北地区盐池县为例, 主要研究目的在于应用新型方法对防护林各树种配置的治沙效应进行分析。另外, 分析并检验了连续风蚀作用下的参数输入变化。结果表明: 单一树种下, 灌木林林内防护效应明显, 乔木林林外防护效应显著; 不同树种配置下, 灌木搭配乔木树种, 在林带背风处, 有效防护范围较小。乔木搭配灌木树种在迎风处能有效的阻止风沙, 但是低矮的乔木树种对上风向的风沙防护效果有限。风沙量累积百分数移动距离表明不同树种配置下的防治风沙效果要好于单一树种。另外, 实验误差小于 3.00%, 并且多次风蚀作用下, 各风沙量百分数移动距离相关性较强, 模型模拟效果较好。

**关键词:** 农田防护林; 指数模型; 累积曲线方法; 风蚀

### 引言

防护林作为人工屏障用途在于减缓风速, 以往防护林用于保护村庄和改善农田景观[1]。作为防护林系统中的重要类型, 农田防护林可以增加动植物种类, 并改善农田系统的生态功能。而且保护土壤免受各侵蚀影响和增加农作物产量[5,15]。因此, 农田防护林建设对实现可持续发展具有重要意义。目前, 对农田防护林的研究, 主要针对在小尺度下防护林的结构配置和结合现有的风蚀模型验证其防护效果两方面。

对防护林结构配置的研究多集中在对林带结构特征及其与环境因子之间的相互关系方面。近些年, 多种方法、研

variables. In recent years, various methods and studies showed that establishing multi-band arbor trees and mesh shrub tree forests within or along the edge of farmlands can provide multiple functions including ecological benefits.

Wind erosion models include theoretical and empirical models. A theoretical model is based on the fluid mechanics principle, with a strong scientific nature founded on the laws of physical movement of sand and provides a superior explanation. The disadvantage and difficulty in developing physical-based models of sand displacement results from the high degree of complexity and randomness, which is a characteristic feature of the mechanical processes of erosion and sediment transport. Hence, the goal of a complete and applicable theoretical model seems unreachable under the given circumstances. Empirical models include the Wind Erosion Equation (WEQ) and the Revised Wind Erosion Equation (RWEQ) models. Different from the theoretical models, empirical models are able to quantify the external factors with minimum assumptions and simple calculations, and provide a wider scope of application. However, with these models, the transport mass must increase without limits for average soil erosion to remain constant for large farm fields; this does not agree with the theory that wind has a limited capacity to transport sand material. This may be true for large farm fields, i.e., there is an increase in transport mass due to the dust carried in suspension, but this portion is relatively small compared with the proportion being transported in suspension, saltation, and creep. While the wind may pick up the surface fine material, the total transport cannot increase without limit [4, 12]. Therefore, empirical models are fundamentally flawed.

At present, scientists and policy makers plan and design farmland shelterbelt forest systems at large scales, i.e., soil erosion control and desertification prevention, from a protection function perspective. Consequently, the rationality of shelterbelt patterns at the landscape scale is a key factor for shelterbelt construction and management. However, the data required for these methods are not easy to obtain, and the methods themselves are difficult to operate, leading to the failure of farmland shelterbelt establishment. Therefore, forestry planners need a reasonable, simple, and easy to operate and control method for the large-scale construction of farmland shelterbelt forests. New methods should overcome the parameter uncertainties and computational complexities in theoretical models as well as the physical defects in empirical models [2]. Meanwhile, a physically-based wind erosion model coupled with empirical functions and methods needs to be developed.

The objective of this study was to use the existing typical farmland shelterbelts as examples to apply a new method to quantitatively analyze the effects of sand prevention and dynamics of sand movement under different arrangements of tree species. In addition, changes in the trends of the input parameters under multiple wind erosion events were analyzed to test their stability and applicability. Our results will provide useful information for supporting the management of farmland shelterbelt forest systems.

## MATERIAL AND METHOD

### Experimental site

The experimental site was located at the Ningxia Yanchi Research Station of the State Forestry Administration (between 37°04'N and 38°10'N, and

研究表明, 在农田中或沿农田边缘营造的带状乔木和网状灌木林分可以提供包括景观生态效益的多种功效功能。

风蚀模型分为理论模型和经验模型。理论模型基于流体力学原理, 建立在风沙物理学运动定律上面, 具有较强的科学性, 并拥有合理解释。而发展基于风沙物理学运动的理论模型缺点和难点在于具有高度的复杂性和不确定性, 这是实际的侵蚀过程和风沙流运动机理内部特性所决定的。因此, 发展完整且可实际应用的理论模型在给定条件下几乎是不可能的。经验模型包括 Wind Erosion Equation (WEQ) 和 Revised Wind Erosion Equation (RWEQ) 模型。不同于理论模型, 经验模型能够量化外界因子以最少的假定条件和简单计算, 提供了较广的适用范围。然而, 这些模型都假定在平均土壤侵蚀作用下, 侵蚀量会一直增加且没有限制, 以确保较大农田范围内侵蚀量为常量。这有悖于理论叙述中的风对风沙的作用能力是有限的。在较大农田范围内, 这也许是对的, 如粉尘被风吹蚀产生悬移使得总风沙量不断被增加。但是悬移颗粒量比例相较于总体的悬移、跃移和蠕移颗粒量比例较小, 风力作用下细小颗粒量可以被吹蚀, 但是总体风沙颗粒量不会无限制增加[4,12]。因此经验模型存在基础性缺陷。

当前, 科研工作者和政策制定者们对农田防护林系统的规划设计, 主要在大尺度下从防护功能角度入手, 例如, 土壤侵蚀控制和风沙防治。所以, 追求景观尺度下合理的防护林样式结构是防护林建设管理的主要目标。然而, 这些方法所需数据在实际过程中不易获取, 且方法本身操作难度较大, 导致防护林体系出现建设失败问题。因此, 对于林业规划者来说, 大规模营造农田防护林需要合理、简单并易操作的风沙防治模型。新方法既要克服理论模型中的参数不确定性、计算的复杂性也要克服经验模型中存在的物理学缺陷[2]。同时需要发展基于风沙物理学模型, 并嵌套经验模型的功能与方法。

本文以现有典型农田防护林为研究对象, 应用新方法, 量化分析了不同树种配置的防护林防沙效应和风沙移动动态过程。另外, 分析了多次风蚀作用下的参数输入的变化来检验模型的稳定性和实用性。本文研究结论可以为农田防护林配置管理提供支持和依据。

## 材料与方

### 研究区概况

实验地点位于中国国家林业局宁夏盐池研究站(北纬 37°04'~38°10'、东经 106°300'~107°410', 海拔为

106°30'E and 107°41'E, with an altitude of 1,354 m above sea level) covering an area of approximately 6,700 km<sup>2</sup>. The annual precipitation averages 287 mm (1950–2010). Mean annual potential evaporation is 1273 mm. Mean annual temperature is approximately 8.1 °C. The prevailing wind is mainly from the northwest, and wind speed averages 3.0 m/s. The landscape is a typical transitional zone; the terrain changes from the Loess to the Ordos plateau. The soils are primarily dark loess soil, eolian sandy soil, and sierozem soil. The vegetation type varies from dry steppe to desert grassland species [6]. The farmland shelterbelt system in the Yanchi semi-arid area is mainly distributed in the flat drought farmland and wind erosion plough land.

### Tree species selection

A survey on the structure of the farmland shelterbelt was conducted in 2009 [14] and 2012. The results of this investigation are as follows:

**Shrub shelter forest:** This is 17-year pure, band shelter forest of *Hedysarum scoparium*. The shelterbelt length and width is 150 m and 40 m, respectively. The average tree height is 2.8 m, and average tree crown width is 1.5 m×2.0 m; *Salix psammophila* is a pure, band shelter forest. The direction of the forest belt runs from northeast to southwest. The length and width of the shelterbelt is 200 and 10 m, respectively, with an average tree height of 2.8 m.

**Arbor shelter forest:** This is a 30-year pure band shelter forest of *Populus bolleana* Lauche; the forest belt direction runs from northeast to southwest; the shelterbelt is 200 m long and 50 m wide with a plant spacing of 4.0 m×4.0 m. The average tree height is 12 m, average diameter at breast height is 0.22 m, average tree crown width is 7.5 m×8.0 m, and average under branch height is 2.5 m. The porosity is 60%; The *Pinus sylvestris* var. *mongolica* stand is at the initial stage of growth. This is a 7-year, mesh shelterbelt forest, with a northeast to southwest direction. The shelterbelt length is 70 m, with a width of 50 m, and a plant spacing of 1.2 m×1.5 m. The average tree height is 2.8 m, average diameter at breast height is 0.27 m, and canopy density is 40%.

Dry farming farmland surrounds the shelterbelt forests. Except for the *Populus bolleana* Lauche forest, the porosity of the tree belts range from 20% to 40%. The survival rate of the shelter forest is determined by the width of the shelterbelt [13] considering the semi-arid and arid climate and the restrictions of land utilization and water resources. Therefore, this article only focuses on the width of the shelter forest (at this time, the protective direction is perpendicular to the wind direction) when determining its influence on wind erosion. In addition, it was assumed that the shelterbelt was complete without any damage and there were no dead trees in the forest. In order to simplify the calculation process, an arrangement of two tree species was considered, and a maximum protective width of 100 m was used.

### Model description

The simulation functions used to characterize the non-uniform displacement of eroded particles were the rational function, simplified Gaussian function and exponential function. Among these three models, the rational function model is limited by mathematical calculations, and the Gaussian function can only simulate the unidirectional distance. For this study, we adopted the exponential model due to its advantages of applicability and reliability in data simulation.

The exponential model has been described by Lobb et

(1950–2010), 占地面积约为 6,700km<sup>2</sup>。年均降水量 287mm (1950–2010), 年均蒸发量 1273mm, 年均气温约为 8.1°C。主风向为西北风, 平均风速为 3.0m/s。地貌景观属于交替区域, 地貌从黄土高原变化至鄂尔多斯平原。土壤类型为黑垆土、风沙土和灰钙土。植被类型从干草原变化至荒漠植被[6]。盐池县沙区农田防护林主要分布在农田集中的平缓干旱沙滩地和风蚀滩地。

### 防护林树种选择

农田防护林分结构调查时间为 2009 年[14]和 2012 年, 调查结果如下:

**灌木防护林:** 花棒 17 年生纯林, 带状防护林, 长 150m, 宽 40m, 平均树高为 2.8m, 平均冠幅为 1.5m×2.0m; 沙柳纯林, 带状防护林, 林带呈东北-西南走向, 带长 200m, 带宽 10m, 平均树高为 2.8m。

**乔木防护林:** 新疆杨 30 年生带状纯林, 林带呈东北-西南走向, 带长 200m, 带宽 50m, 株行距为 4.0m×4.0m, 平均树高为 12m, 平均胸径为 0.22m, 平均冠幅为 7.5m×8.0m, 平均枝下高为 2.5m。林带疏透度为 60%; 樟子松林分处于生长初期, 为 7 年生网状防护林, 林带呈东西—南北走向, 带长 70m, 带宽 50m, 株行距为 1.2m×1.5m, 平均树高为 2.8m, 平均胸径为 0.27m, 郁闭度为 40%。

各防护林带周围为平坦开阔的沙质旱作农田。除新疆杨林外, 其它防护林疏透度在 20%到 40%。防护林带宽度是决定防护林存活率的重要决定因素[13]。考虑到在半干旱、干旱地区气候条件和受制于土地利用、水资源限制, 因此, 本文只针对防护林宽度(此时防护林方向与风向成垂直方向)对风蚀作用的影响分析, 并假定防护林带无破损、树木无死亡情况出现, 为了简化计算过程, 对 2 种树种进行配置组合, 最大防护距离为 100m。

### 模型描述

模拟功能可以模拟可蚀性颗粒的不均匀分布状态, 有: 有理函数模型、简化的高斯模型和指数模型。在这三种模型, 有理函数模型在数理学计算上存在局限性。高斯模型只能模拟风沙流在单一水平下的移动距离。本文采用指数模型, 优点是在数据模拟、预测拥有更好的适用性和可靠性。

al. [10]. The exponential model used to simulate the non-uniform displacement of eroded particles under multiple wind erosions is:

$$\frac{C_{(x)}^{S*}}{C_u} = 1 - D_w^* e^{-\frac{x}{D_w}}, [\%] \quad (1)$$

where:  $C_u$  is the total amount of sand,  $x$  is the sand displacement distance (m),  $C_{(x)}^{S*}$  is the amount of sand at  $x$  after wind erosion, and  $D_w$  is the ratio of the windblown depth and eroded soil depth, with a value of 1.  $D_w$  is the wind erosion model coefficient (defined as an average sand displacement distance (m)).

This model assumes that the extent of sand translocation is infinite (the series of distributions is summed to generate a summation curve,  $c_s$ ); this extent is described experimentally as the extreme point at which applied eroded particles can be measured above background levels. The data generated by the exponential model can be used with the summation curve method to quantify the sand prevention effect.

Summation Curve Method: The methods used to calculate the summation curve are described by Lobb and Kachanoski [8, 9, 11]. In this paper, the summation curve method was improved for application to wind erosion studies. Eroded particles under wind erosion events were measured using established methods, i.e., the estimated eroded particle distribution for a series of sequential hypothetical sand sources with a length exceeding the maximum distance to which particles were transported was used to generate a summation curve to calculate the mean eroded particle movement in the windblown direction (Fig.1a). Using the summation curve method, the mean eroded particle distance per unit width and the average eroded depth ( $D_w$ ) was calculated using the following equation (2):

$$D_w = \int_0^\infty (1 - c_s) dx, [m] \quad (2)$$

The summation curve was used to quantify the dispersion of the eroded particles. Three steps were used in this process. First, the areas above and below the summation curve, delineated by  $x=0$ , were used to calculate  $u_{s1}$ :

$$u_{s1} = \sqrt{\frac{(\int_{-\infty}^0 c_s x^2 dx + \int_0^\infty (1 - c_s) x^2 dx - \int_{-\infty}^0 (c_s x dx)^2 + \int_0^\infty (1 - c_s) x dx)^2}{C}}, [m] \quad (3)$$

Second, the areas above and below the summation curve, delineated by  $x=D_w$ , were used to calculate  $u_{s2}$  (Fig.1b):

$$u_{s2} = \int_{D_w}^\infty (1 - c_s) dx, [m] \quad (4)$$

Third, the cumulative percentiles of the eroded particles amount were calculated.  $D_{W50}$ ,  $D_{W75}$ ,  $D_{W90}$  and  $D_{W95}$  correspond to the 50<sup>th</sup>, 75<sup>th</sup>, 90<sup>th</sup>, and 95<sup>th</sup> cumulative percentiles of the amount of eroded particle displacements respectively (Fig. 1b).

To characterize the general form of the distribution of eroded particles,  $u_{s1}$  and  $u_{s2}$  were expressed as relative measures of  $D_w$ ,  $u_{s1,2}$  (%):

本文采用 Lobb[10]对指数模型描述, 可模拟连续风蚀下可蚀性颗粒的不均匀移动距离分布, 公式为:

式中,  $C_u$  为风沙总量,  $x$  为风沙移动距离 (m),  $C_{(x)}^{S*}$  为风蚀后在  $x$  距离处的风沙量,  $D_w^*$  为吹蚀深度与可蚀性土壤层深度比, 值为 1;  $D_w$  为风蚀模型系数 (定义为风沙平均移动距离 (m))。

指数模型假定风沙移动量是趋于无限的 (累积比例量为  $c_s$ ), 并描述在风力作用下所有被吹蚀的颗粒移动距离大于起始位置处。将指数方程产生的模拟数据代入到累积曲线方法中, 可以对防沙效果进行定量分析。

累积曲线方法: 累积曲线方法由 Lobb 和 Kachanoski[8,9,11]提出, 本文中, 累积曲线方法被改进以应用至风蚀研究中。在风蚀作用下, 采用累积量计算方法, 例如, 在风蚀方向下, 假设一系列相同的风沙源被吹蚀, 直到可蚀性颗粒移动至最大距离, 此时对风蚀方向下的可蚀性颗粒量累积加和计算, 得到累积曲线 (图 1a)。因此,  $D_w$  代表颗粒物在平均风蚀宽度和深度下的平均移动距离, 计算公式 (2):

累积曲线方法可以用于量化可蚀性风沙颗粒分布过程, 分为三步计算过程: 第一步从  $x=0$  处计算风沙颗粒分布过程, 得到  $u_{s1}$ :

第二步, 当风蚀颗粒移动至平均移动距离 ( $x=D_w$ ),  $u_{s2}$  计算公式为 (图 1b):

第三步, 风沙量累积百分数计算,  $D_{W50}$ ,  $D_{W75}$ ,  $D_{W90}$  和  $D_{W95}$  分别代表累积百分数 50%, 75%, 90%和 95%的风沙量移动距离 (图 1b)。

区分对颗粒物一般性分布过程的描述, 可将计算出的  $u_{s1}$  和  $u_{s2}$  与实际输出值  $D_w$  比较, 得到计算误差  $u_{s1,2}^*$  (%), 公式为:

$$u_{s1,2}^* = 100 \times \frac{u_{s1,2}}{D_W}, [\%] \tag{5}$$

The first and second steps still take the general form of the distribution of the amount of sand particles based on the empirical results. Consequently, for the actual calculations,  $u_{s1}^*$  and  $u_{s2}^*$  should equal 100% of  $D_W$  and 50% of  $D_W$ .

$D_W$  can also be converted directly to mass,  $D_M$  (kg/m), which is the eroded particle mass per unit width:

$$D_M = s\rho D_W, [\text{kg/m}] \tag{6}$$

where:  $\rho$  is bulk density ( $\text{kg/m}^3$ ).  $s$  is wind erosion width (m).

第一种和第二种计算方式仍采用基于经验模型结果的风沙颗粒一般性分布描述。所以，在实际计算中， $u_{s1}^*$  和  $u_{s2}^*$  应该分别接近于 100% 的  $D_W$  值和 50% 的  $D_W$  值。

$D_W$  也可以转换为风沙侵蚀量  $D_M$  (kg/m)，为风蚀作用宽度侵蚀量：

式中  $\rho$  为容重 ( $\text{kg/m}^3$ )。  $s$  是风蚀作用宽度 (m)。

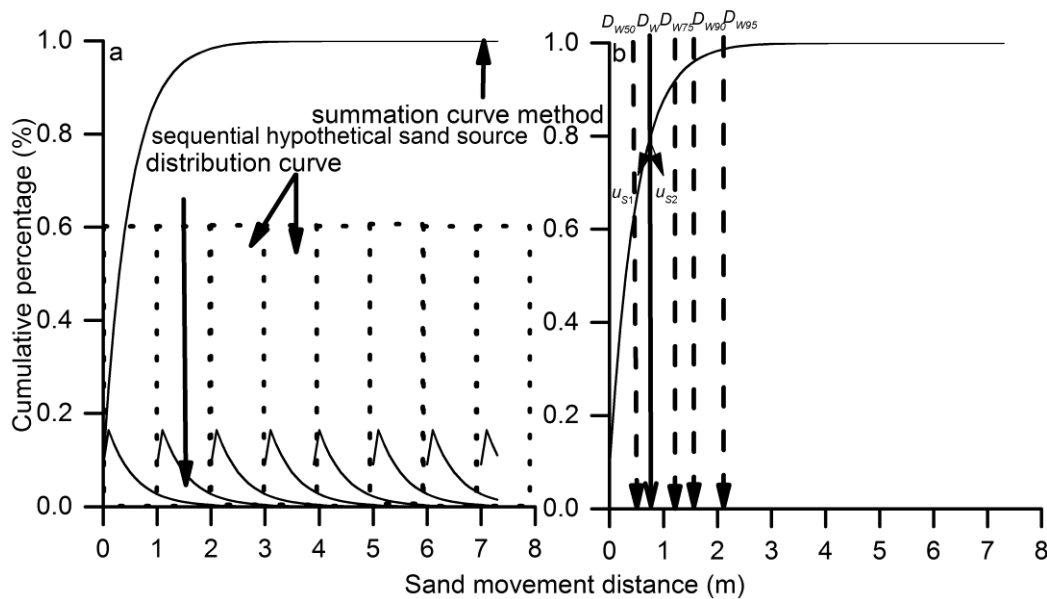


**Fig.1** - Summation Curve Method. a) Sand source: sand before wind erosion is indicated by the dotted line ( $L_P= 1.00$  m); sand after wind erosion is indicated by the distribution line below; the summation curve represents the accumulation of sand ( $D_W= 0.50$  m; top line above). b) Dispersion is indicated by  $D_{W50}$ ,  $D_{W75}$ ,  $D_{W90}$ , and  $D_{W95}$ , i.e., the cumulative percentile of the particles along the path of 50%, 75%, 90%, and 95% displacement, respectively. Arrows represent sand movement to a distance of  $D_W$  where  $u_{s2}$  was calculated

The magnitude of the undulations on the summation curve,  $\epsilon$  (m), was calculated over a distance equal to  $L_P$  (m), beyond the distance to which the eroded particles were observed,  $L_S$  (m). The coefficient of the experimental error and translocation variability ( $\epsilon^*$ ) was estimated as:

$$\epsilon^* = \left( \frac{\int_{L_S}^{L_S+L_P} |1 - c_s| dx}{D_W + L_P} \right) \times 100, [\%] \tag{7}$$

where:  $L_P$  is sand source (m),  $L_S$  is maximum sampling distance (m).

Theoretically, the summation curve should increase steadily from  $x = 0$  to its maximum at  $L_S+L_P$  and then decrease steadily to a value of zero. However, the summation curves generated from experimental data are not smooth; rather, they undulate (Fig. 2a). These undulations are a result of experimental errors. Therefore, experimental errors exist.  $\epsilon$  is a measure of the inherent variability in translocation (Fig. 2b). Hence,  $\epsilon$  is referred to as the experimental error.

累计曲线方法计算会产生波动，波动距离  $\epsilon$  是在风沙颗粒移动距离等于或超过  $L_P$  处并在  $L_S$  (m) 处计算、观测得到的，实验误差及变异程度  $\epsilon^*$  表示为公式：

式中  $L_P$  为风沙源距离 (m)， $L_S$  为最大风沙采样距离 (m)。

理论上，累积曲线从  $x=0$  处上升，直到移动至最大距离  $L_S+L_P$ ，然后平稳下降至 0。然而，源于实验数据计算得到的曲线方程并非是一条平滑的直线，相反，会产生波动 (图 2a)。这些波动是由于实验内部误差造成的，因此，实验误差一直存在，由于  $\epsilon$  为实验内部系统性存在结果 (图 2b)。所以  $\epsilon^*$  可认定为是实验误差。

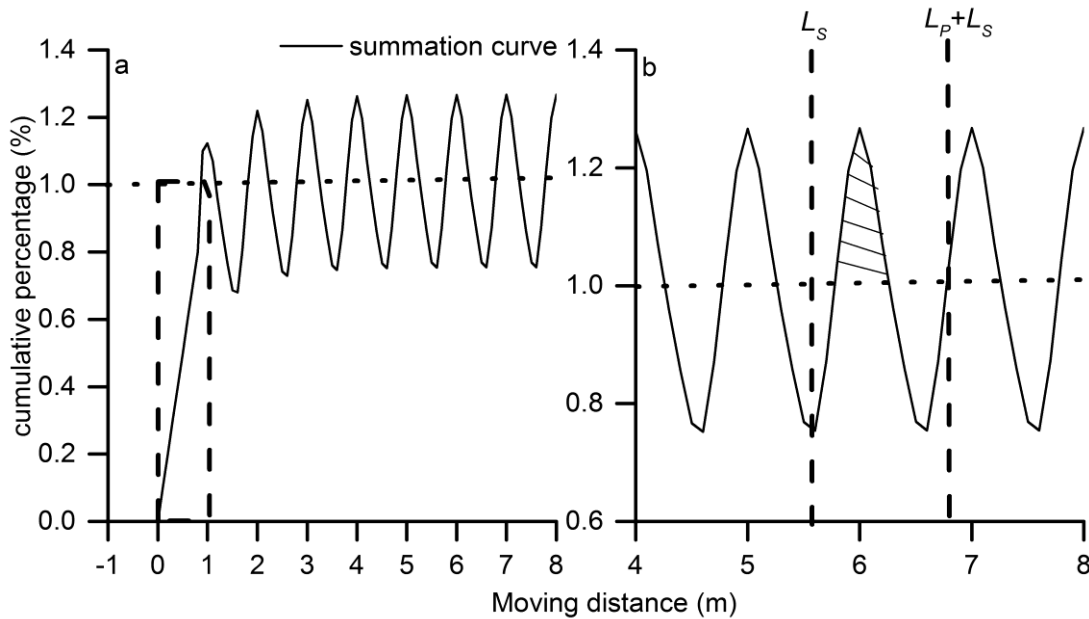


Fig.2 - Experimental error demonstration: a) Sand source: sand before wind erosion is indicated by the dotted line ( $L_P=1.00$  m,  $D_W=0.50$  m); b)  $\epsilon$  for the summation curve method, represented by the hatched area ( $L_P=1.00$  m,  $L_S=5.70$  m)

$D_W$  was calculated under different tree species arrangements using the following:

不同树种配置下的  $D_W$  计算公式见:

$$D_W = \frac{D_{W-tree\ species\ A} + D_{W-tree\ species\ B}}{n}, [m] \tag{8}$$

where:  $D_{W-tree\ species\ A, B}$  is the average sand displacement distance (m) of the shelter tree species A and B. The value of  $D_W$  was determined as the mean of  $D_{W-tree\ species\ A}$  and  $D_{W-tree\ species\ B}$ .

式中  $D_{W-tree\ species\ A, B}$  是防护林树种 A 和 B 的林内风沙平均移动距离 (m)。总  $D_W$  的计算为防护林树种 A 和 B 的风沙移动距离的平均值。

**RESULTS**

**Outside forest sand source parameter input selection**

In this study, it was assumed that all sand particles originated from outside the forest (bare sandy land, no shelter forest) and were distributed within the farmland shelterbelts. Therefore, we defined the outside forest farmland as sand sources and the shelter belts as storage sinks. This paper focuses on sand with a moving distance less than or equal to 100 m; therefore, the sand source parameter input should ensure that the average sand moving distance is greater than 50 m (the boundary between tree species A and B), and that the largest moving distance exceeds 100 m from the outer boundary. Here, the diameter of the outside forest sand source was set as 100 m, the sampling point interval was 1 m, the sand bulk density was 1100 kg/m<sup>3</sup> and the wind erosion depth was 0.0010 m. The distribution pattern of the eroded particles was simulated by applying the exponential model, and then the  $D_W$  value was obtained using the summation curve method. The optimal parameter was selected when  $D_W$  was 60 m, 50% of the accumulated amount of sand concentrated around a distance of 50 m, and the largest moving distance exceeded 100 m (Fig. 3).

**结果**

**林外风沙源参数输入选择**

本文假定所有风沙颗粒来自于林外 (裸沙地, 无防护林), 并最终分布在农田防护林内。因此, 林外裸沙地设定为源, 防护林林内为汇。本研究只考虑 100m 范围内的风沙移动走向。因此, 在林外风沙源参数输入上, 应确保风沙源风沙移动平均距离大于 50m (树种 A 和 B 的配置边界), 外边界最大移动距超过源内 100m。在本文中, 设定林外风沙源直径距离为 100m, 采样点为 1m, 风沙容重为 1100kg/m<sup>3</sup>。土壤层吹蚀深度为 0.0010m。指数方程提供风沙分布模拟值, 代入到累计曲线方法中, 得到各参数  $D_W$  输出值。图 3 为参数筛选后得到最佳参数输入值, 当  $D_W$  为 60m 时, 50%的累积风沙量集中在 50m 处, 最大移动距离超过 100m (图 3)。

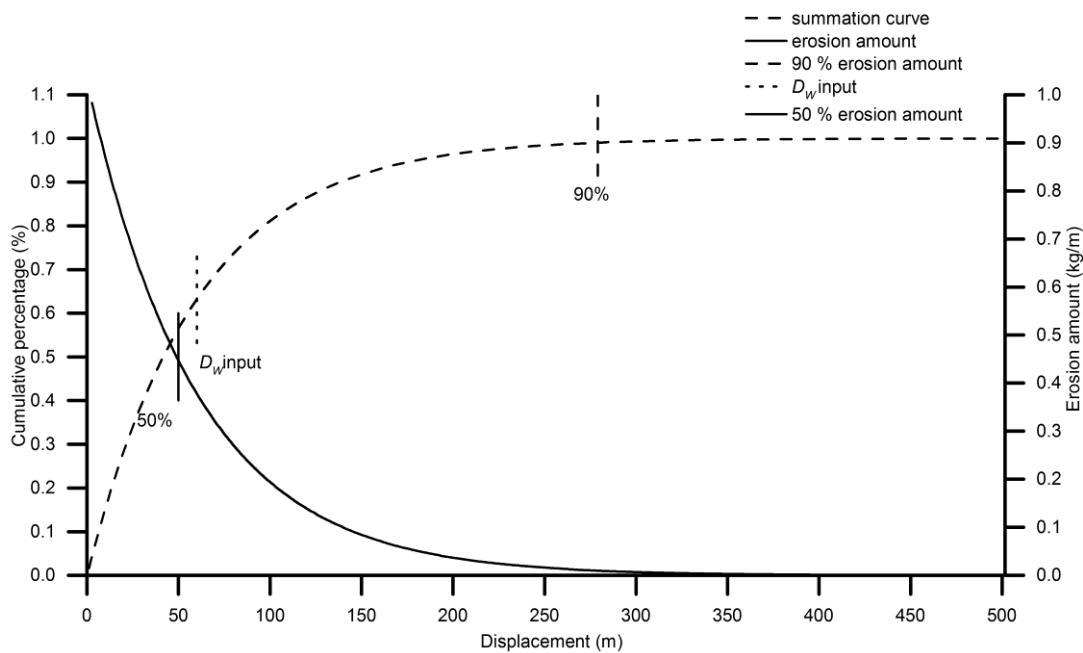


Fig.3 - Estimation of the wind erosion rate based on the summation curve method associated with 50 % and 90 % of total sand moving distance when  $D_w$  equaled 60 m

#### Effects of different arrangements of shelterbelt tree species

Previous studies indicated that the ventilation coefficients of *Hedysarum scoparium*, *Salix psammophila*, and *Pinus sylvestris* var. *mongolica* shelter forests belonged to a tight structure with ventilation coefficients of 0.2. In contrast, the *Populus bolleana* Lauche shelter forest had a loose structure with a ventilation coefficient of 0.3 [7]. The effective sand prevention distances (outside forest) were 0.5 H for *Hedysarum scoparium*, 1 H for *Salix psammophila*, 4 H for *Populus bolleana* Lauche, and 2 H for *Pinus sylvestris* var. *mongolica*. The effective sand prevention distances (inside forest) were 4 H, 2 H, 0.5 H, and 1 H for *Hedysarum scoparium*, *Salix psammophila*, *Populus bolleana* Lauche, and *Pinus sylvestris* var. *mongolica*, respectively [14].

Thus, the value of the sand moving distance within the *Populus bolleana* Lauche shelter forest was set at 6 m. The  $D_w$  values of *Hedysarum scoparium*, *Salix psammophila*, and *Pinus sylvestris* var. *mongolica* were set at 2 m, 4 m, and 8 m, respectively, according to different ventilation coefficients, and  $L_p$  was 1 m, and the sand sampling point was 0.1 m.

Under the single arrangement of tree species, the shrub shelter forest could not prevent sand movement outside the forest belt, but effectively prevented sand movement within the forest belt (table 1). The arbor forest effectively prevented wind erosion outside the forest. However, such a prevention effect was not obvious inside the forest.

The results of different tree species arrangements indicated that when the shrub tree species was arranged with the arbor tree species, there were vast quantities of sand accumulation on the lee side of the shelterbelt. Although the sand prevention effect was better than a single tree species, the effect was insignificant. An arbor forest with shrub tree species can effectively prevent most of the sand on the windward side, but was associated with a higher calculation error. However, short arbor trees with shrub tree species such as *Pinus sylvestris* var. *mongolica* could not provide effective

#### 不同防护林树种配置效应

以往研究表明,花棒、沙柳和樟子松林为紧密结构,对应通风系数为 0.2,新疆杨为疏散结构,对应的通风系数为 0.3[7]。各树种的林外的阻沙效应为 0.5H(花棒)、1 H(沙柳)、4H(新疆杨)和 2H(樟子松);林内的阻沙效应分别为 4H(花棒)、2H(沙柳)、0.5H(新疆杨)和 1H(樟子松)[14]。

因此,本文设定新疆杨林的林内风沙移动距离为 6m。根据通风系数的比例计算得出花棒、沙柳和樟子松的  $D_w$  值输入分别为 2m, 4m 和 8m。本文中  $L_p$  设置为 1m, 风沙采样点设置为 0.1m。

单一树种下,灌木林未能有效阻止外部的风沙源,但是能有效的阻止林内风沙的移动。乔木林可以有效的阻止林外风沙侵蚀。然而,林内阻沙效应并不明显(表 1)。

不同树种配置结果表明,灌木搭配乔木树种,在防护林带背风处,风沙大量堆积,虽然比单一树种配置要好,但是防风蚀效果不显著。乔木搭配灌木树种在迎风处能有效的阻止绝大部分的风沙,但是计算误差较高。然而,低矮的乔木林搭配灌木树种,如樟子松不能对外部的风沙源形成有效的防护。

累积曲线方法能够计算得到风沙吹蚀分布中产生的实验

protection to external sand sources.

The numerical procedures used to calculate eroded particle displacement resulted in errors. Under a single tree species arrangement, the *Pinus sylvestris* var. *mongolica* shelter forest showed the highest error of 1.40%. Under a different tree species arrangement, the *Populus bolleana* Lauche shelter forest was associated with the highest error of 2.97%. The main reason for these errors is that sand loss was calculated using the exponential model. In this research, the calculation error was controlled within 3.00% under conditions where was assumed that experimental errors were negligible and the results were satisfactory.

For the hypothetical data,  $\dot{u}_{S1}^*$  and  $\dot{u}_{S2}^*$  were lower than the average  $D_w$ . This is due to the fact that these measures relate to the general form of the distribution of eroded particles. As the form of the distribution approached that of a step,  $\dot{u}_{S1}^*$  approached a value of 100% and  $\dot{u}_{S2}^*$  approached a value of 50%, which agree with the previous equations mentioned above.

误差。单一树种配置下，樟子松防护林的计算误差最高，为 1.40%。不同树种配置下，新疆杨与各树种防护林配置下的计算误差最高，为 2.97%。造成误差的主要原因是，指数方程计算下产生的风沙损失量。本研究中，计算误差被控制在 3.00% 以内，认为实验误差可以忽略，计算结果较为满意。

对于模拟数据输出值， $\dot{u}_{S1}^*$  和  $\dot{u}_{S2}^*$  要小于  $D_w$ ，这是由于其计算方式仍然采用一般性风蚀颗粒的分布描述。作为其分布描述步骤， $\dot{u}_{S1}^*$  更接近实际值的 100% 和  $\dot{u}_{S2}^*$  接近实际值的 50%，这与之前的模型计算公式描述结果一致。

Table 1

$D_w$  input, values of  $D_w$  calculated using the summation curve method associated with experimental errors

Tree species arrangement	$D_w$ input	$D_w$ output	$\dot{u}_{S1}^*$	$\dot{u}_{S2}^*$	$\epsilon$
	[m]	[m]	[%]	[%]	[%]
H*	2.00	1.99	79.86	50.54	0.95
S*	4.00	3.99	65.89	45.08	0.91
B*	6.00	5.99	84.67	36.78	1.26
P*	8.00	7.99	77.13	37.08	1.40
HS	-	2.41	83.03	44.07	0.67
HP	-	3.02	78.99	42.89	0.69
HB	-	2.05	98.23	50.46	0.92
SH	-	2.42	97.22	49.27	0.65
SP	-	5.72	87.53	40.85	1.22
SB	-	4.61	97.66	39.67	1.03
B,HSP	-	1.12	98.32	49.69	2.97
PH	-	6.12	78.94	40.81	1.32
PS	-	6.15	87.70	41.01	1.33
PB	-	6.19	92.45	40.71	1.34

\* H represents *Hedysarum scoparium*, S represents *Salix psammophila*, B represents *Populus bolleana* Lauche, P represents *Pinus sylvestris* var. *Mongolica*

Amount of eroded particle dispersion (50%, 75%, 90%, and 95%) expressed as percentiles of cumulative translocation can provide useful information for understanding wind erosion and the dynamics of sand movement.

Figure 4 shows that greater sediment deposition occurred on the lee side of the arbor trees, and the potential of wind erosion was higher than with shrub tree species. Complete shelter belts (tall trees), such as *Populus bolleana* Lauche, had the greatest sand prevention effect, while incomplete shelter belts (short trees), such as *Pinus sylvestris* var. *Mongolica*, did not exhibit a clear sand prevention effect. In general, the combination of different tree species showed a better sand prevention effect than a single shelter forest.

风沙量百分数移动分布（50%、75%、90%和 95%）能更好理解风蚀作用和风沙移动的动态过程提供有效信息。

图 4 表明，乔木林在背风处严重积沙，并且其潜在风蚀率要高于灌木树种。完整的防护林带（高大的乔木树种），如新疆杨防护林对于风沙防治效应效果最为明显。但是不完整的防护林带（低矮的乔木树种），如樟子松防护林，防治风沙效果并不明显。总体来说，不同树种组合下的防治风沙效果要好于单一树种下的防护林配置。



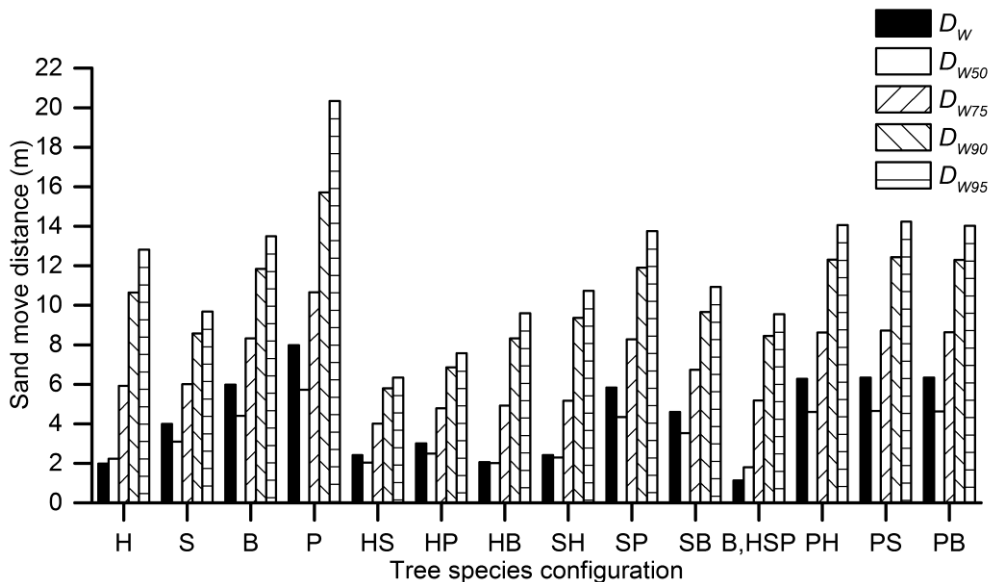


Fig.4 - Bars of different shelter tree species combinations indicated by  $D_{W50}$ ,  $D_{W75}$ ,  $D_{W90}$ , and  $D_{W95}$  represent the 50, 75, 90, and 95% cumulative percentiles, respectively, of the amounts of sand along the path of displacement

**Sand loss**

Sand loss was estimated using the exponential model. In general, small amounts of sand loss are associated with a low experimental error in the summation curve method. Figure 5 shows that there was a positive correlation between sand loss and the  $D_W$  input. Sand loss with *Pinus sylvestris* var. *mongolica* was 3 times that of a single tree species and 6 times that of different tree species arrangements. But this difference was considered insignificant. In theory, only when the  $D_W$  value exceeds the maximum distance ( $L_S$ ) will calculation results generate significant error [3]. Therefore,  $L_S$  should be set as far as possible. In addition, for accurate measurement of sand displacement,  $L_P$  should be set as short as possible, at least 1 m, and the sand sampling interval should be set to least 0.1 m to filter out this undulation (error). Consequently, a smoother summation curve will be generated, which can provide better results.

**风沙损失量**

指数方程用来估算风沙损失量。一般而言，较小的损失量带入到累计曲线方法中产生误差也较小。图 5 看出， $D_W$  输入值与损失量成一定程度的正相关。樟子松树种配置上风沙的损失量分别是单树种损失量的 3 倍和不同树种配置损失量的 6 倍。但是差异并不显著。理论上，只有当  $D_W$  值超过最大的距离  $L_S$  时，计算结果会造成较大误差 [3]。因此  $L_S$  值应尽量设置较远。另外，为准确计算风沙移动距离， $L_P$  应设置较小，至少为 1m，并且风沙采样点设置至少为 0.1m，这样可以过滤掉波动带来的实验误差。因此，计算得到的累计曲线会更加平滑，可提供较为理想的实验结果。

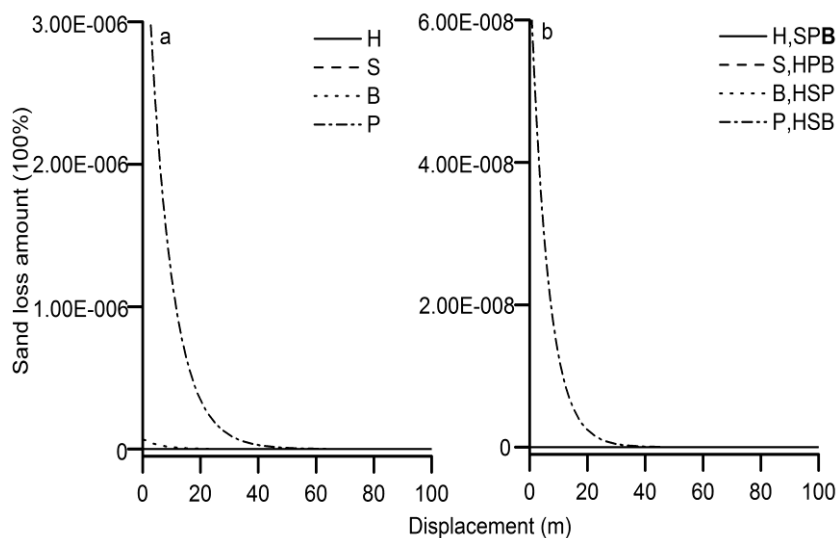


Fig.5 - Sand losses of different shelter tree species  
 a) Sand loss of a single tree shelterbelt.  
 b) Sand loss of a different arrangement of trees species

**Multiple wind erosion process analysis**

Wind erosion can significantly affect the underlying surface. For the purpose of long-term planning of sand prevention, it is essential to analyze these effects under multiple wind erosion events. As discussed above, the exponential function can simulate the distribution of eroded particles under a continuous wind erosion process, and the summation curve method can determine the dynamics of sand movement. Therefore, the data generated by the exponential model can be understood as the process of sand movement under continuous wind erosion events or multiple years of wind erosion. In this paper, *Pinus sylvestris* var. *mongolica* and *Hedysarum scoparium* trees were selected to demonstrate the process of sand movement under 5 continuous wind erosion events. Figure 6 shows that under a constant  $D_W$  parameter input, the output values were stable; a small amount of sand loss did not affect the simulation results. Linear regression analysis indicated that there was strong correlation between sand movements under multiple wind erosion events, whereas  $R^2$  decreased with an increase in the cumulative percentage. Theoretically, during multiple wind erosion events, the cumulative percentage of the sand moving distance should show a decreasing trend due to the shelter forest controlling the wind effect. In general, the summation curve is stable and accurate, and can be used as a mid- or long-term protective model.

**连续风蚀过程分析**

风蚀作用能显著影响下垫面，作为长期防治风沙的重要手段，分析多次风蚀作用对于下垫面的影响效果是十分必要的。以上研究表明，由于指数方程可以模拟可蚀性颗粒在连续多次的风蚀下的分布过程，累计曲线模型可计算可蚀性颗粒动态运动分布过程。因此，指数方程计算的连续风蚀过程下的可蚀性颗粒运动过程也可以理解为连续或连年的风蚀过程下的可蚀性颗粒分布过程。本文中，以花棒和樟子松分析为例，在连续 5 次风蚀作用下，分析可蚀性颗粒的移动过程。图 6 表明，在相同的  $D_W$  参数输入下，指数方程计算参数输出稳定，少量风沙损失量并未影响模拟效果。线性回归分析结果表明，多次风蚀作用下的风沙移动数据相关程度较强， $R^2$  随移动距离百分比增大而减小。理论上，受制于防护林防风效果，风沙量移动百分比移动距离应呈减小趋势。总体上，累积曲线模型计算方法稳定程度较高，较为精确，可作为防护林中长期的防护模型。

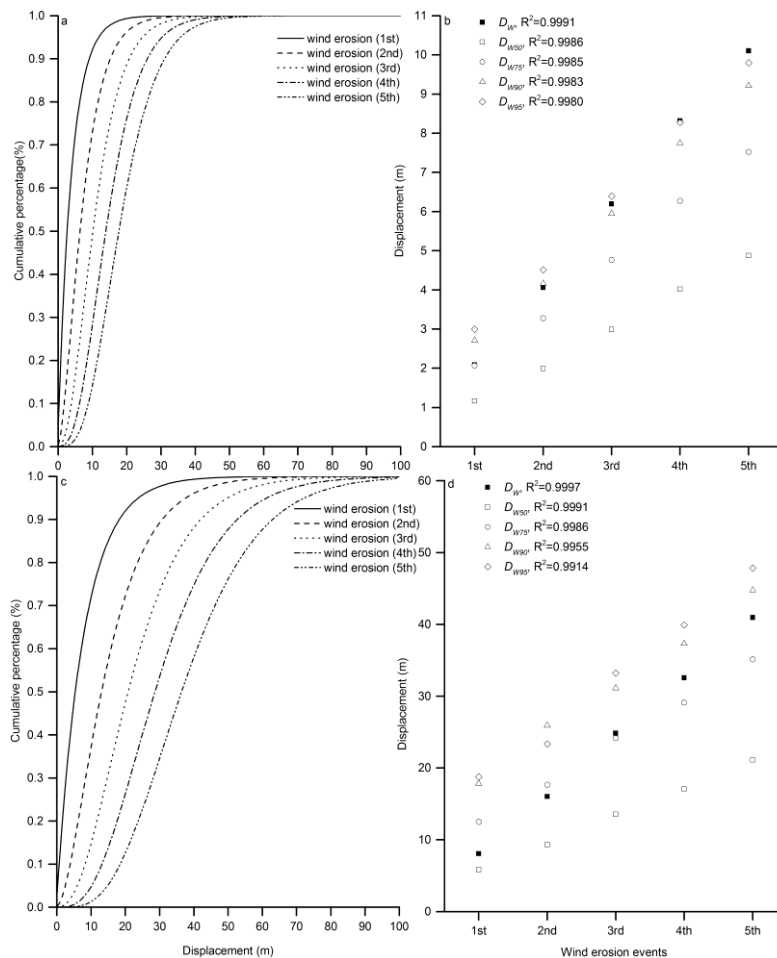


**Fig. 6** - Analysis of multiple wind erosion events. (a, b) Sand source (inside forest) changing trend (using *Hedysarum scoparium* as an example) and linear relationship of the  $D_{W50}$ ,  $D_{W75}$ ,  $D_{W90}$ , and  $D_{W95}$  values. (c, d) Sand source (inside forest) changing trend (using *Pinus sylvestris* var. *mongolica* as an example) and linear relationship of the  $D_{W50}$ ,  $D_{W75}$ ,  $D_{W90}$ , and  $D_{W95}$  values

## DISCUSSIONS AND CONCLUSIONS

The ultimate goal of wind erosion research is to establish erosion models that can predict particle erosion losses at different temporal and spatial scales. In general, the scientific and practical explorations of wind erosion studies are rather limited; therefore, it is a necessary to rebuild the theoretical based method for a wider application.

Based on former studies, this paper proposed a new method of analysing the effects of sand prevention in a shelterbelt forest. Because it is difficult to obtain accurate data, this paper used general conclusions from previous studies as estimates. The results indicated that experimental errors were well controlled and the conclusions drawn from the final analysis indicate that this method can provide direction and idea for shelterbelt management.

Compared with the empirical model, the summation curve method accounts for the fundamental theories of physical principles of blown sand and sedimentation processes. In addition, the theoretical model is more complicated than the summation curve due to the numerical calculations. Thus, the summation curve is the best method.

In the actual calculation and application, the summation curve method has two advantages. The first is that the input parameters are simple; the second is that this method can be used at different scales. Therefore, the summation curve can be applied to a wider scope when assessing farmland protection forest.

Considerable work needs to be conducted in future research. In this study, the assessment method was based on a single direction (width of the belts). However, different areas vary with respect to the topography, land use, degree of wind erosion and other factors, and these factors interact with each other. Therefore, it is necessary to establish a classification standard in future studies.

An additional decision factor in the design of optimal farmland shelterbelt systems involves the water requirements of the tree species because water is a limited resource and may be the main factor that prevents long-term maintenance of farmland shelterbelt systems in arid or semi-arid regions. Further studies are required to determine the water consumption of shelter forest tree species and the local water resources to explore the best afforestation density and shelterbelt forest structure.

## ACKNOWLEDGEMENT

This work was supported by the National Basic Research Program of P. R. China (2013CB429906); National "Twelfth Five-Year" Plan for Science & Technology Support (2012BAD16B02); The Commonwealth Project of State Forestry Administration of P. R. China (201304325)

## REFERENCES

- [1]. Brandle J.N., Hodges L., Zhou X.H., (2004) – *Windbreaks in North American agricultural systems*, Agroforestry Systems, vol.61, no.1/3, pp.65-78;
- [2]. Cleugh H.A., (1998) – *Effects of windbreaks on airflow, microclimates and crop yields*, Agroforestry Systems, vol.41, no.1, pp.55-84;
- [3]. Dale A., Passi G.R., (2012) – *Modeling dust emission caused by wind erosion*, Journal of Geophysical

## 讨论与结论

风蚀研究最终目标是建立能够预测不同时间尺度和不同地表类型的风蚀模型。一般而言，过去对风蚀研究的探索兼顾科学性和实用性较少。因此，重新构建具有理论基础与更广泛适用性的风蚀模型势在必行。

本文在现有防护林研究基础上，加入了新的研究方法，分析了防护林防治风沙效果。因为计算所需要的精确数据获取难度大，故本文采用前人研究中的一般结论进行估算。研究表明，实验误差被较好的控制，并且最终分析得到的结论可以为防护林建设管理提供新的研究方向和思路。

对比经验模型，累积曲线方法采用了风沙吹蚀沉降的基础物理学理论。另外，理论模型较累积曲线方法在数理计算上要更加复杂。因此累积曲线方法要优于以上模型。

实际计算、应用上，累积曲线方法具有两方面优势，一是输入参数简单；二是可以应用至各个尺度。因此，累积曲线方法可以应用至更大范围内的农田防护林评估。

下一步需要进行的工作是，本文只考虑单一方向的风蚀效应（防护林带的宽度）。然而，不同地区的地形、土地利用、风蚀率和其他相关因子也不尽相同，并且这些因子相互作用影响。因此未来的工作需要将这些因子进行分类研究。

另外，需要考虑的因素是在设计最优化合理的农田防护林时将农田防护林树种的水分利用情况考虑进来，因为在干旱和半干旱地区，受制于水资源限制，水分是阻碍农田防护林系统长期维持的主要因素。未来工作也需要结合防护林各树种蒸腾耗水规律和当地水资源条件，研究探讨最佳防护林造林密度和结构。

## 致谢

国家重点基础研究发展计划项目（2013CB429906）、“十二五”国家科技支撑计划项目（2012BAD16B02）、国家林业局公益性行业科研专项（201304325）。

## 参考文献

- [1]. Brandle J.N., Hodges L., Zhou X.H. (2004) – *北美农田系统的防风林带研究*, 农田森林系统, 第 61 卷, 第 1/3 期, 65-78;
- [2]. Cleugh H.A. (1998) – *防风林带对气流、微气候和农作物产量的影响*, 农田森林系统, 第 41 卷, 第 1 期, 55-84;
- [3]. Dale A., Passi G.R. (2012) – *风蚀作用下的粉尘释放*

Research: Atmospheres, vol.93, no.11, pp.14233-14242;

[4]. Fryrear D.W., Bilbro J.D., Saleh A., Schomberg H., Stout J.E., Zobeck T.M., (2000) – *RWEQ: Improved wind erosion technology*, Journal of Soil and Water Conservation, vol.55, no.2, pp.183-189;

[5]. Fukuda Y., Moller H., Burns B., (2011) – *Effects of organic farming, fencing and vegetation origin on spiders and beetles within shelterbelts on dairy farms*, New Zealand Journal of Agricultural Research, vol.54, no.3, pp.155-176;

[6]. Guanglei Gao, Guodong Ding, Yuanyuan Zhao, Wei Feng, Yanfeng Bao, Ziwei Liu., (2014) – *Effects of Biological Soil Crusts on Soil Particle Size Characteristics in Mu Us Sandland*, Transactions of the Chinese Society for Agricultural Machinery, vol.45, no.1, pp.115-120;

[7]. Juan E.P., Daniel E.B., Ted M.Z., (2010) – *Comparison of different mass transport calculation methods for wind erosion quantification purposes*, Earth Surface Processes and Landforms, vol.35, no.13, pp.1548-1555;

[8]. Lobb D.A., Kachanoski R.G., Miller M.H., (1995) – *Tillage Translocation and Tillage Erosion on Shoulder Slope Landscape Positions Measured Using Cs-137 as a Tracer*, Canadian Journal of Soil Science, vol.75, no.2, pp.211-218;

[9]. Lobb D.A., Kachanoski R.G., (1999) – *Modelling tillage erosion in the topographically complex landscapes of southwestern Ontario, Canada*, Soil and Tillage Research, vol.51, no.3-4, pp.261-277;

[10]. Lobb D.A., Kachanoski R.G., (1995) – *Modelling tillage translocation using step, linear-plateau and exponential functions*, Soil and Tillage Research, vol.51, no.3-4, pp.317-330;

[11]. Lobb D.A., Quine T.A., Govers G., Heckrath G.J., (2001) – *Comparison of methods used to calculate tillage translocation using plot-tracers*, Journal of Soil and Water Conservation, vol.56, no.4, pp.321-328;

[12]. Mao Y., Wilson J.D, Kort J., (2013) – *Effects of a shelterbelt on road dust dispersion*, Atmosphere Environment, vol.79, pp.590-598;

[13]. Mohammed A.E., Stigter C.J., Adam H.S., (1996) – *On shelterbelt design for combating sand invasion*, Agriculture Ecosystems & Environment, vol.57, no.2-3, pp.81-90;

[14]. Qiang Cui, Jiarong Gao, Mingyue He, Zhanguang Zhao, Jinrui Zhang., (2009) – *Effects of farm land shelterbelts in controlling wind and sand in sandy land of Yanchi*, Journal of Ecology and Rural Environment, vol.25, no.3, pp.25-29;

[15]. Wiseman G., Kort J., Walker D., (2009) – *Quantification of shelterbelt characteristics using high-resolution imagery*, Agriculture Ecosystems and Environment, vol.131, no.1/3, pp.111-117.

模型, 地球物理学研究, 第 93 卷, 第 11 期, 14233-14242;

[4]. Fryrear D.W., Bilbro J.D., Saleh A., Schomberg H., Stout J.E., Zobeck T.M. (2000) – *RWEQ: 风蚀模型的改进*, 水土保持学报, 第 55 卷, 第 2 期, 183-189;

[5]. Fukuda Y., Moller H., Burns B. (2011) – *乳牛场防护林内的有机耕作、围犁和基于蜘蛛和甲壳虫的植被覆盖的效果研究*, 新西兰农业研究, 第 54 卷, 第 3 期, 155-176;

[6]. 高广磊, 丁国栋, 赵媛媛, 冯薇, 包岩峰, 刘紫薇. (2014) – *生物结皮发育对毛乌素沙地土壤粒度特征的影响*, 农业机械学报, 第 45 卷, 第 1 期, 115-120;

[7]. Juan E.P., Daniel E.B., Ted M.Z. (2010) – *量化分析风蚀为目的, 对比不同风蚀颗粒吹蚀的计算方法*, 地貌变化与地理地形, 第 35 卷, 第 13 期, 1548-1555;

[8]. Lobb D.A., Kachanoski R.G., Miller M.H. (1995) – *利用 Cs-137 为示踪物测量肩坡地形下的耕作过程和耕作侵蚀率*, 加拿大土壤科学, 第 75 卷, 第 2 期, 211-218;

[9]. Lobb D.A., Kachanoski R.G. (1999) – *加拿大安大略省南部复杂地形地貌下的耕作侵蚀模型*, 土壤和耕作研究, 第 51 卷, 第 3-4 期, 261-277;

[10]. Lobb D.A., Kachanoski R.G. (1995) – *耕作过程模型分析, 以逐步回归、线性回归和幂指数函数为例*, 土壤和耕作研究, 第 51 卷, 第 3-4 期, 317-330;

[11]. Lobb D.A., Quine T.A., Govers G., Heckrath G.J. (2001) – *利用大田示踪物对比不同耕作过程的研究方法*, 水土保持学报, 第 56 卷, 第 4 期, 321-328;

[12]. Mao Y., Wilson J.D, Kort J. (2013) – *公路防护林对粉尘的作用影响*, 大气环境, 第 79 卷, 第 4 期, 590-598;

[13]. Mohammed A.E., Stigter C.J., Adam H.S. (1996) – *以阻碍风沙为目的的防护林设计方法*, 农业生态系统与环境, 第 57 卷, 第 2-3 期, 81-90;

[14]. 崔强, 高甲荣, 何明月, 赵哲光, 张金瑞. (2009) – *宁夏盐池沙地农田防护林的防风阻沙效益*, 生态与农村环境学报, 第 25 卷, 第 3 期, 25-29;

[15]. Wiseman G., Kort J., Walker D. (2009) – *利用高分辨率影像对防护林特性进行量化分析*, 农业生态系统与环境, 第 131 卷, 第 1/3 期, 111-117.